

Organic & Biomolecular Chemistry

Accepted Manuscript



This is an *Accepted Manuscript*, which has been through the Royal Society of Chemistry peer review process and has been accepted for publication.

Accepted Manuscripts are published online shortly after acceptance, before technical editing, formatting and proof reading. Using this free service, authors can make their results available to the community, in citable form, before we publish the edited article. We will replace this *Accepted Manuscript* with the edited and formatted *Advance Article* as soon as it is available.

You can find more information about *Accepted Manuscripts* in the [Information for Authors](#).

Please note that technical editing may introduce minor changes to the text and/or graphics, which may alter content. The journal's standard [Terms & Conditions](#) and the [Ethical guidelines](#) still apply. In no event shall the Royal Society of Chemistry be held responsible for any errors or omissions in this *Accepted Manuscript* or any consequences arising from the use of any information it contains.

Cite this: DOI: 10.1039/c0xx00000x

www.rsc.org/xxxxxx

ARTICLE TYPE

σ -Hole $\cdots\pi$ and Lone Pair $\cdots\pi$ Interactions in Benzylic Halides[†]

Teresa Montoro,^c Gloria Tardajos,^b Andrés Guerrero,^b María del Rosario Torres,^d Cástor Salgado,^a Israel Fernández,^{*a} and José Osío Barcina^{*a}

Received (in XXX, XXX) Xth XXXXXXXXX 20XX, Accepted Xth XXXXXXXXX 20XX

DOI: 10.1039/b000000x

Intermolecular and intramolecular halogen $\cdots\pi$ interactions in benzyl halides (Ph-CR₂-X; X = F, Cl, Br and I) derived from 7-phenylnorbornane were investigated. The imposed geometry of the 7-arylnorbornane moiety prevents the participation of intramolecular attractive interactions between the σ -hole region of the halogen atom and the π electrons of the aromatic ring. Crystallographic data show intermolecular halogen bonds in iodide **1** and bromide **2** in the solid state. On the other hand, both UV-Vis and D-NMR data suggest the occurrence of intramolecular interactions between the halogen atoms and the phenyl rings in these compounds in solution. To provide more insight into the nature of the observed stabilizing interactions, density functional calculations were also carried out. These computations confirm the presence of genuine lone pair $\cdots\pi$ intramolecular interactions which strongly affect the stability and the electronic structure of these species.

Introduction

Among the large number of non-covalent interactions, both halogen bonds¹⁻⁴ and lone pair $\cdots\pi$ interactions⁵⁻⁸ have attracted considerably attention in recent years, not only because of their intriguing nature but also because of their applications in supramolecular chemistry, crystal engineering and material science,⁹⁻¹⁶ bioorganic chemistry and biochemistry,¹⁷⁻²³ and inorganic chemistry.²⁴

The stabilizing nature of halogen bonds is somewhat surprising since it involves the attractive interaction between two electron rich atoms (RX \cdots B; B = N, O; X = F, Cl, Br, I) or regions (RX $\cdots\pi$ systems). However, this "like-like" interaction can be interpreted in terms of the σ -hole concept, a localized positive region of electrostatic potential placed on the surface of the halogen atoms.^{2,25} This positive region explains the high directionality observed in intermolecular halogen-bonded systems (RX \cdots B angles close to 180° or T-shaped arrangements in the case of RX $\cdots\pi$ interactions), since σ -holes are placed along the extensions of the R-X bonds. However, besides electrostatic interactions, dispersion and induction forces and charge-transfer interactions have been described as important contributions to halogen bonding.²⁶⁻³³

So far, lone pair $\cdots\pi$ (LP $\cdots\pi$) interactions have been mostly studied with oxygen and nitrogen atoms acting as donors and electron poor aromatic systems.^{5-8,34} The study of these weak interactions in the case of halogen atoms is particularly difficult due to their strong tendency to interact *via* their σ -hole. As a result, very few examples of halogen bonds that avoid the σ -hole and are based on genuine $n\rightarrow\pi^*$ interactions have been described.³⁵ In that respect, the design of model systems that allow the study of halogen interactions where the σ -hole contribution is hampered (or not possible) is highly desirable.

Herein we describe our experimental, spectroscopic and computational investigations on the nature of the inter- and intramolecular non-covalent interactions between halogen atoms and aromatic π -systems in benzylic halides.

Results and Discussion

For this study we have chosen a series of 7-aryl-7-halonorbornanes as model compounds **1-4**, easily obtained from the corresponding alcohols following standard procedures (Figure 1). Several reasons account for this choice. Most of the studies on halogen $\cdots\pi$ bonds carried out until now are based on intermolecular interactions where the interacting subunits can adopt a T-shaped arrangement with the σ -hole of the halogen atom pointing directly towards the π electrons of the donor moiety. 7-Aryl-7-halonorbornanes allow the study of intermolecular halogen bonds as well as intramolecular X $\cdots\pi$ interactions without participation of the σ -hole region since the angles between the C-X bonds and the aryl ring do not allow this interaction.³⁶ On the other hand, the most stable conformation in 7-arylnorbornanes is the perpendicular one, because the H-*exo* hydrogen atoms of the norbornane structure hinder the rotation of the phenyl ring. Therefore, in these derivatives the intramolecular X $\cdots\pi$ interaction is favoured by the preorganization of the substrates. Preorganized 7-arylnorbornanes have been successfully used to study aromatic face-to-face and edge-to-face interactions, C-H $\cdots\pi$ and O-H $\cdots\pi$ interactions, as well as in the design of stable supramolecular complexes with Ag⁺ and NH₄⁺ ions.³⁷⁻⁴¹

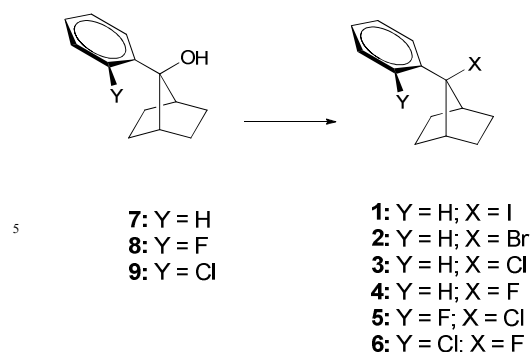


Figure 1 Synthesis of benzylic halides **1-6**. Reaction conditions: **1:** 7/NaI/BF₃·OEt₂/CH₃CN (86%); **2:** 7/PBr₅/CH₂Cl₂ (82%); **3 (or 5):** 7 (or **8**)/SOCl₂ (98% or 95%); **4 (or 6):** 7 (or **9**)/DAST/CH₂Cl₂ (93% or 95%).

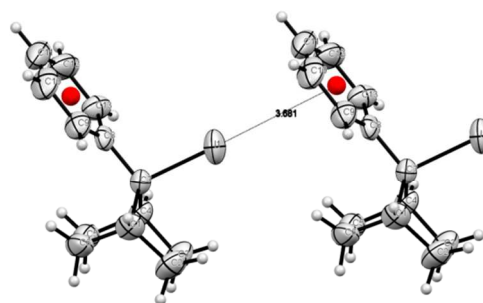


Figure 2 Crystal structure of iodide **1** showing the intermolecular I... π halogen bond.

Crystal structures

Single-crystal X-ray measurements were accomplished for solid compounds **1-3** (Figures 2-4). The crystal structures of iodide **1** and bromide **2** show similar patterns and the crystal packing in both cases is characterized by the presence of C–I... π and C–Br... π halogen bonds that lead to the formation of infinite 7-aryl-7-halonorbomane chains. The X... π (centroid) distances (**1:** 3.68 Å; **2:** 3.59 Å) are shorter than the sum of the van der Waals radii of the involved atoms (I = 2.15 Å; Br = 1.95 Å) and the phenyl group (1.7 Å).

The angles surrounding iodine (C₇–I–Ph_{centroid} = 178.3°; C₁₁–Ph_{centroid}–I = 78.4°) and bromine (C₇–Br–Ph_{centroid} = 176.6°; C₁₁–Ph_{centroid}–Br = 80.1°) are in agreement with the high directional character of halogen bonds. In the case of bromide **2**, the Br... π distance is closer to the sum of the van der Waals radii (Δ = 0.06 Å) than in the case of iodide **1** (Δ = 0.17 Å), thus suggesting that the X... π interaction is stronger when iodine atoms are involved.

The crystal structures of **1** and **2** are noteworthy because, although halogen bonds with aromatic systems are well documented and established,⁴² those involving phenyl rings are relatively rare. Thus, a search of the structures of benzylic iodides (83 hits with phenyl rings) deposited in the Cambridge Structural Database (CSD) (Figures S1 and S2, supplementary information) shows that there are very few halogen bonds in these crystal structures, whose packings are dominated by hydrogen bonds, halogen...halogen interactions and/or π -stacking interactions. As an example, no halogen bonds are observed in the crystal structure of 1,4-bis(iodomethyl)benzene.⁴³ Moreover, the I...phenyl distance observed in **1** is one of the shortest described to date and only in one single case a shorter contact (3.58 Å) has been reported.⁴⁴

The situation observed in benzyl bromides is very similar. CSD data (504 hits) (Figures S3 and S4, supplementary information) show that short Br... π contacts are observed only in a limited number of structures and as an example, in 1,4-bis(bromomethyl)benzene and similar benzyl bromides no Br... π halogen bonds are observed.^{45,46} Furthermore, a

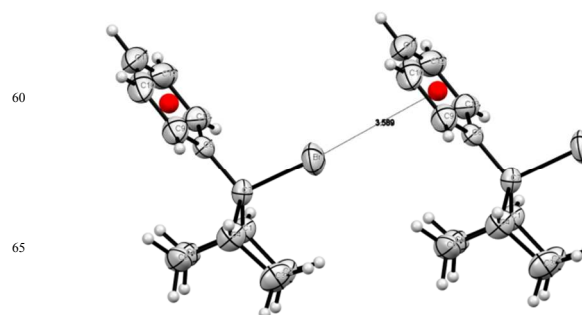


Figure 3 Crystal structure of bromide **2** showing the intermolecular Br... π halogen bond.

comprehensive statistical analysis of the crystal structures deposited in the CSD published very recently⁴⁷ reveals that halogen bonds with phenyl rings are found frequently, but when the halogens are Br, Cl or F hydrogen bonding interactions between the aryl ring edge and the halogens are dominant. Only in the case of iodine, halogen... π interactions are more frequent than hydrogen bonds. It should be also noted that only a small fraction of the halogen-phenyl contacts studied (32% for Br and 14% for I) are shorter than the corresponding sum of the van der Waals radii.⁴⁷

By contrast, the crystal structure of chloride **3** (Figure 4) shows a different pattern than that described for **1** and **2**. Instead of a Cl... π bond, a CH... π interaction is observed in this case. The CH₁₁–Ph_{centroid} distance is 2.89 Å, just in the limit of the sum of the van der Waals radii for hydrogen and a phenyl ring (1.20 Å and 1.70 Å, respectively). Therefore, from the data obtained from the crystal structures of the halides **1**, **2** and **3**, it can be concluded that the strength of the non-covalent interactions studied increases in the order I... π > Br... π > CH... π > Cl... π .

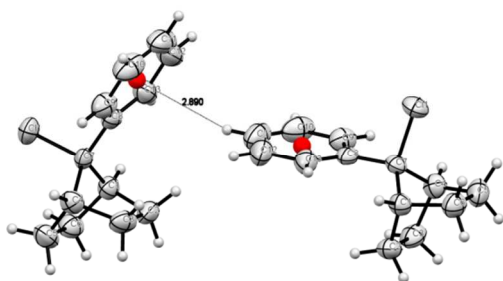


Figure 4 Crystal structure of chloride **3** showing the intermolecular CH \cdots π interaction.

Spectroscopic studies

UV-Vis spectroscopy is an important tool for the study of interactions in solution. In the case of those involving halogen atoms, it has been described that UV-Vis spectra provide direct information about the interactions of dihalogens with aromatic compounds⁴⁸ and halogenated organic molecules with halide anions.⁴⁹ Thus, the formation of complexes between diiodine and dibromine with benzene are characterized by the appearance of new absorption bands in the UV-Vis spectra centered at 285 nm.⁴⁸ Despite these early studies, UV-Vis spectroscopy has not been recently applied to understand the nature of halogen bonds involving aromatic donors.

In order to gain more insight into the halogen \cdots π interactions in our model compounds, we have recorded the corresponding absorption spectra. The UV-Vis spectra of benzylic halides **1-4** are depicted in Figure 5 whereas the main absorptions are shown in Table 1. All four halides show strong bands at short wavelengths (< 200 nm) characteristic of the benzene $\pi \rightarrow \pi^*$ allowed transition (β or 1B_b band) (see Figure S5, supplementary information).⁵⁰ In addition, a second absorption is observed between 200 and 260 nm. These bands show a bathochromic shift on going from fluoride **4** to iodide **1** (**4**: 205 nm; **3**: 219 nm; **2**: 230 nm; **1**: 230 nm). The origin of this bands is not clear since the p (or 1L_a) band of monoalkylbenzenes is observed around 204–207 nm.^{50,51} The weak forbidden α (1L_b) bands can be observed in fluoride **4** and chloride **3** between 230–270 nm and are overlapped by the transitions centered at 230 nm in bromide **2** and iodide **1**. Finally, iodide **1** shows an additional band at 276 nm. It is well-known that the UV-Vis spectra of alkyl iodides show absorption bands due to $n \rightarrow \sigma^*$ transitions around 260 nm. Thus, the band for *t*-butyl iodide is observed at 269 nm and in the case of isopropyl iodide at 262 nm.⁵² However, the molar extinction coefficients of these forbidden transitions are very low ($\epsilon < 600$), while in the case of iodide **1** the ϵ value is 2300 L \cdot mol $^{-1}\cdot$ cm $^{-1}$ and the band is bathochromically shifted (276 nm) in comparison with alkyl iodides. The analogous $n \rightarrow \sigma^*$ in alkyl bromides appears at about 208 nm ($\epsilon \sim 300$ L \cdot mol $^{-1}\cdot$ cm $^{-1}$), and at < 200 nm in alkyl chlorides and fluorides. Finally, non-significant differences of the spectral features of all four halides

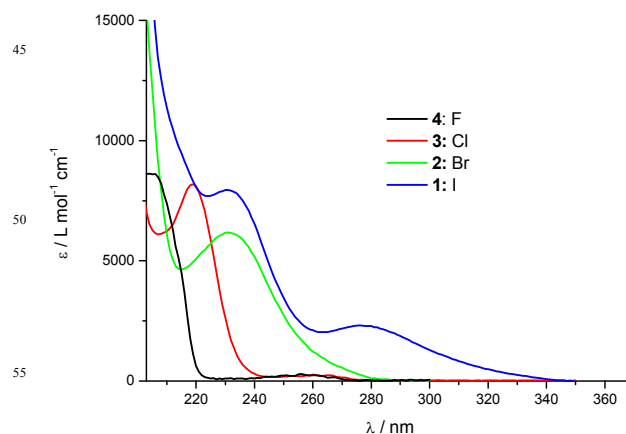


Figure 5 UV-Vis spectra of benzylic halides **1-4** in dilute hexane solution at 298 K.

Table 1 Comparison of main UV/Vis excitation energies (λ_{max} , hexane) of benzylic halides **1-4**.

Compound	$\lambda_{\text{exp}} / \text{nm}^a$	$\lambda_{\text{calc}} / \text{nm}^b$	Transition ^c
1	230 (7800)	243 (0.18)	HOMO-3 \rightarrow LUMO
	276 (2300)	293 (0.08)	HOMO \rightarrow LUMO
2	230 (6200)	243 (0.18)	HOMO \rightarrow LUMO (66%) ^c HOMO-3 \rightarrow LUMO (21%) ^c
3	219 (8200)	221 (0.16)	HOMO \rightarrow LUMO
4	205 (8400)	209 (0.06)	HOMO \rightarrow LUMO

^a λ_{exp} recorded in dilute hexane solution at 298 K. Values in parenthesis indicate the corresponding ϵ (in M $^{-1}\cdot$ cm $^{-1}$). ^b Computed PCM(*n*-hexane)-TD-B3LYP/def2-TZVPP//M06-2X/def2-TZVPP vertical excitation energies. Values in parenthesis indicate the corresponding oscillator strengths. ^c Transition contribution.

have been observed within the range of $10^{-6} - 10^{-3}$ mol L $^{-1}$ in hexane at 298 K, which points to the absence of intermolecular aggregation processes.

In view of these results, some of the bands observed in halides **1-4** may be tentatively assigned to a charge transfer interaction between the aryl ring and the halogen atoms, as a consequence of intramolecular X \cdots π bonding. The distances between the halogen atoms and the C $_{\text{ipso}}$ of the phenyl ring, according to the crystal structures, are below the sum of the van der Waals radii (**1**: 2.95 Å vs. 3.85 Å; **2**: 2.79 Å vs. 3.65 Å; **3**: 2.66 Å vs. 3.50 Å). Furthermore, these should be LP \cdots π interactions since the σ -holes of the halogens are directed outside the planes of the aromatic rings.

To clarify the nature of the electronic transitions responsible for the observed absorptions in the respective UV-Vis spectra, a time-dependent (TD)-DFT study was carried out. The computed vertical transitions and corresponding oscillator strengths show a nice agreement with the experimental data

(see Table 1). For compounds **4** and **3**, the observed absorption at $\lambda_{\max} = 205$ and 219 nm, respectively, is the result of the one-electron promotion from the HOMO (which mainly involves the π -aryl fragment) to the LUMO (see Figure 6). This HOMO→LUMO transition is steadily redshifted when going down in the halogens group (from 205 nm in **4** to 276 nm in **1**). The corresponding molar extinction coefficient steadily decreases as well (from 8400 $\text{M}^{-1}\text{cm}^{-1}$ in **4** to 2300 $\text{M}^{-1}\text{cm}^{-1}$ in **1**). Therefore, these results indicate that the differential absorption exhibited by iodine species **1** appears at 230 nm. This new absorption corresponds, according to our TD-DFT calculations, to the HOMO-3→LUMO vertical transition. Strikingly, as readily seen in Figure 6, the HOMO-3 is a delocalized orbital which involves the π system of the aromatic ring and also the p atomic orbital of the iodine atom. Therefore, a clear intramolecular LP $\cdots\pi$ interaction is present in this species and not in compounds **3** and **4**, which agrees with the strength of the non-covalent interactions commented above. A similar delocalized molecular orbital, which is responsible for the occurrence of a homoconjugation band, has been found in closely related 7-diarylnorbornanes.^{37,53-55} This HOMO-3→LUMO transition occurs in compound **2** as well. However, in this case the corresponding LP- π band overlaps with the HOMO→LUMO transition and the observed band is the result of the combination of both transitions according to our TD-DFT calculations (Table 1).

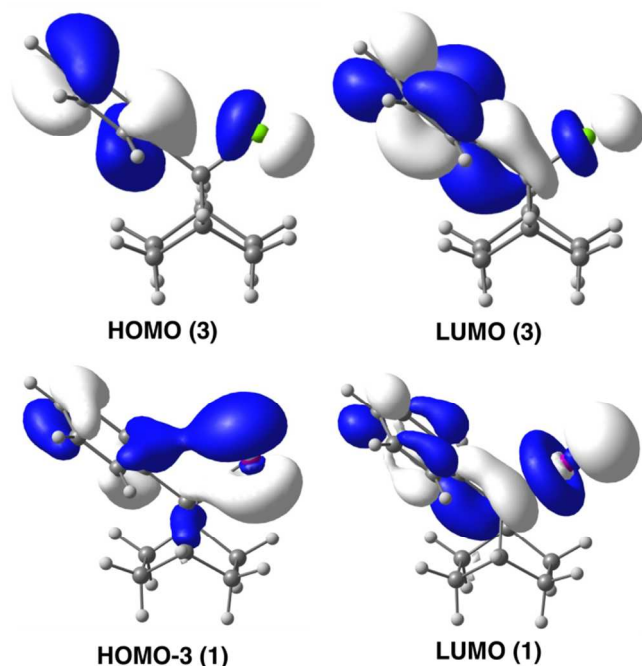


Figure 6 Computed molecular orbitals compounds **3** (top) and **1** (bottom) (isosurface value of 0.04 a.u.).

At this point, it would be highly desirable to find experimental evidence of the LP $\cdots\pi$ interactions found by our

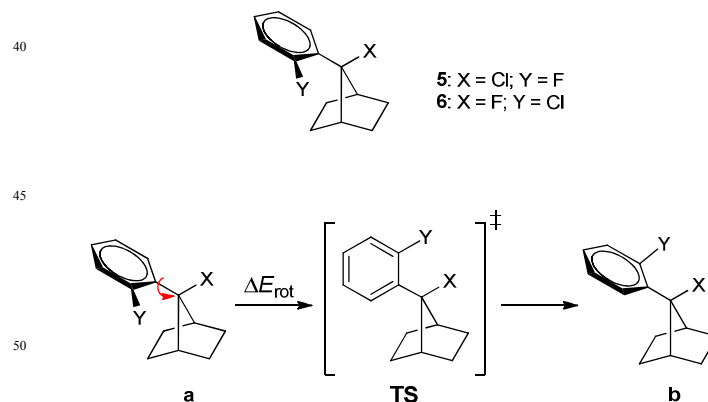


Figure 7 Conformations of benzylic halides **5** and **6**.

computational calculations. With this idea in mind, we decided to study the rotational barriers of 7-arylnorbornanes **5** and **6** (Figure 7). An important advantage of this type of compounds is that the rotational barriers of the phenyl rings provide valuable information about the energies and the non-covalent interactions present in these species.^{37,39} The rotational barriers can be easily measured by D-NMR introducing substituents (Y) in the *ortho* position of the phenyl ring and analyzing the coalescence of the bridgehead protons. The values of these rotational barriers represent the energy difference between the most stable perpendicular conformation **a** and the planar conformation in the corresponding transition state, **TS** (ΔE_{rot} in Figure 7). Thus, stabilization of conformation **a** increases the rotational barrier, while stabilization of conformation **TS** exerts the opposite effect.^{37,39} When X or Y are halogen atoms heavier than Cl, the rotational barriers are too high to be determined ($T_c > 150^\circ$) due to steric hindrance. Despite that, the results obtained in this work for compounds **5** and **6** are highly significant. Thus, for the benzyl halide **6**, a barrier of 11.3 kcal mol^{-1} was measured, whereas a much higher rotational barrier of 18.3 kcal mol^{-1} was determined in the case of halide **5**. A possible explanation of this energy difference is that **5a** is more stabilized than **6a** by a Cl $\cdots\pi$ interaction, which is known to be stronger than the F $\cdots\pi$ interaction present in **6a**.^{17,29,56}

DFT calculations carried out at the dispersion-corrected M06-2X/def2-TZVPP level⁵⁷ confirms that **5a** is indeed 2.6 kcal mol^{-1} more stable than **6a** (Figure 8). Interestingly, our calculations, which match the rotational barriers measured experimentally ($\Delta G_{298}^\ddagger = 10.6$ and 19.4 kcal mol^{-1} for **6** and **5**, respectively), indicate that the transition state associated with the rotation of **6a**, **TS1**, is much more stable than that involving **5a** ($\Delta\Delta G_{298}^\ddagger = 6.2$ kcal mol^{-1}). This can be mainly ascribed to the higher Pauli repulsion between the lone-pairs of the halogen atoms in **TS2** as a consequence of a shorter F \cdots Cl distance (2.625 Å vs 2.646 Å, see Figure 8). Reasons for this

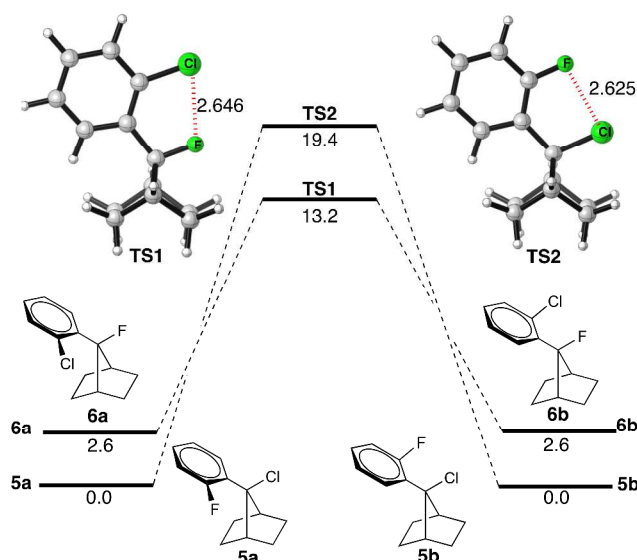


Figure 8 Computed reaction profile for the rotational process involving **5a** and **6a**. Free energies (computed at 298 K) and bond distances are given in kcal mol⁻¹ and angstroms, respectively. All data have been computed at the M06-2X/def2-TZVPP level.

remarkable difference between both saddle points are not clear at this moment.

The different stability of the equilibrium geometries of **5** and **6** can be explained with the help of the Natural Bond Orbital (NBO) method.⁵⁷ Thus, the second-order perturbation theory (SOPT) of the NBO method locates a stabilizing electronic donation from an atomic *p* orbital of the halogen atom (i.e. a lone-pair) to a π^* molecular orbital of the aryl fragment in **5** and **6** (see Figure 9, left). Interestingly, the associated SOPT-energy, $\Delta E^{(2)}$, is clearly higher in **5** than in **6** ($\Delta E^{(2)} = -1.63$ and -1.22 kcal mol⁻¹, respectively), thus confirming the higher strength of the Cl $\cdots\pi$ interaction compared to the F $\cdots\pi$ interaction. A similar $\pi-\pi^*$ homoconjugated interaction was found by us in related 7-diarylnorbanes,^{54,55} therefore indicating that the preorganized geometry of 7-arylnorbornanes allows the electronic communication between atoms or groups with available donor π -orbitals with the π^* system of the aryl fragment. In addition, the SOPT method also locates a stabilizing donation from a π molecular orbital of the aryl fragment to the $\sigma^*(\text{C-X})$ molecular orbital (Figure 9, right). Similar to the halogen $\cdots\pi$ interaction, this additional, stabilizing $\pi\rightarrow\sigma^*$ interaction is stronger in **5** than in **6** ($\Delta E^{(2)} = -6.88$ and -5.92 kcal mol⁻¹, respectively), thus contributing to the higher stability of **5**.⁵⁸

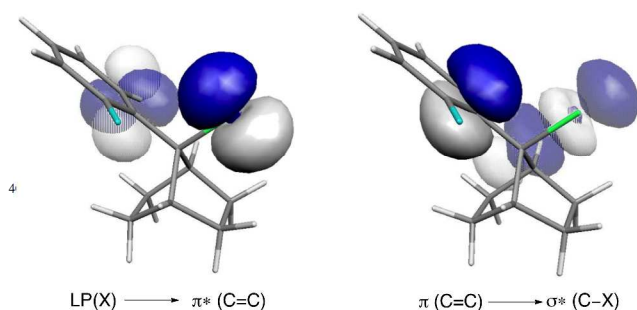


Figure 9 Natural Bond Orbitals responsible for the stabilizing interactions in compounds **5** and **6**.

Conclusions

The benzylic halides studied in this work show intermolecular halogen bonds in the cases of iodide **1** and bromide **2** in the solid state. Crystallographic data indicate that this bond is particularly strong in **1**, that exhibits one of the shortest I $\cdots\pi$ (phenyl) distances reported to date (3.68 Å). The strength of the intermolecular non-covalent interactions in our compounds increases in the order I $\cdots\pi$ > Br $\cdots\pi$ > CH $\cdots\pi$ > Cl $\cdots\pi$.

On the other hand, in solution UV-Vis and D-NMR data as well as computational calculations provide evidence on the existence of intramolecular halogen $\cdots\pi$ interactions in our model compounds. These halogen mediated bonds are not based on the interactions of the σ -holes of the halogen atoms and the phenyl rings since the geometry of benzylic halides prevents these contacts. Indeed, these bonds can be considered as the result of a charge transfer from the lone pair of the halogens to the π^* orbital of the adjacent phenyl ring. This genuine LP $\cdots\pi$ interaction is particularly remarkable in iodide **1** and, as a consequence, a new absorption derived from the HOMO-3 \rightarrow LUMO vertical transition appears in the corresponding UV-Vis spectrum ($\lambda_{\text{max}} = 230$ nm). In addition, these $n\rightarrow\pi^*$ (LP $\cdots\pi$) interactions play an important role in the rotational barriers as well as in the stability of benzylic halides.⁵⁹

Computational Details

All the calculations reported in this paper were obtained with the GAUSSIAN 09 suite of programs.⁶⁰ All compounds were optimized using the Truhlar's meta hybrid exchange-correlation functional M06-2X, which is useful for describing non-covalent interactions,⁶¹ in combination with the triple- ζ quality def2-TZVPP basis sets, which are supposed to be close to the DFT basis set limit.⁶² All species were characterized by frequency calculations and have positive definite Hessian matrices. Transition structures (TS's) show only one negative eigenvalue in their diagonalized force constant matrices, and their associated eigenvectors were confirmed to correspond to the motion along the reaction coordinate under consideration. Calculations of absorption spectra were accomplished by using the time-dependent density functional theory (TD-DFT)⁶³

method with the B3LYP⁶⁴ functional and taking into account solvent effects (*n*-hexane) by means of the Polarizable Continuum Model (PCM).⁶⁵ This level is denoted PCM(*n*-hexane)-TD-B3LYP/def2-TZVPP//M06-2X/def2-TZVPP. The B3LYP Hamiltonian was chosen because it was proven to provide reasonable UV/Vis spectra for a variety of chromophores.⁶⁶ The assignment of the excitation energies to the experimental bands was performed on the basis of the energy values and oscillator strengths. Donor–acceptor interactions were computed by using the natural bond orbital (NBO) method.⁶⁷ The energies associated with these two-electron interactions were computed according to the following equation:

$$\Delta E_{\phi\phi}^{(2)} = -n_{\phi} \frac{\langle \phi^* | \hat{F} | \phi \rangle^2}{\epsilon_{\phi^*} - \epsilon_{\phi}}$$

Experimental

Materials and methods

¹H and ¹³C NMR spectra were recorded on a 300 MHz spectrometer. Chemical shifts are given in ppm relative to TMS (¹H, 0.0 ppm) and CDCl₃ (¹³C, 77.0 ppm). Coupling constants are given in Hertz. The rotational barriers of compounds **5** and **6** were determined by variable-temperature experiments in a 300 MHz spectrometer in tetradeuterio-1,2-dichloroethane. Absorption spectroscopy experiments were carried out at 298 K, in hexane (concentration of ca. 10⁻⁵ mol L⁻¹), using quartz cuvettes with optical paths of 1 cm. UV-Vis spectra were recorded using an UVICON XL spectrophotometer (Bio-Tex Instruments). All experiments involving organometallic reagents were carried out under argon atmosphere using standard Schlenk techniques. Anhydrous solvents were distilled under argon following standard procedures. Flash chromatography was performed over silica gel 60 (230-400 mesh). All commercially available compounds were purchased from commercial suppliers and used without further purification. The preparation of alcohols **7**, **8** and **9** was carried out according to a described procedure.^{37,39} Alcohols **7** and **8** and chloride **3** have been described elsewhere.^{37,55}

Compound 1: To a stirred mixture of 500 mg (2.66 mmol) of **7** and 399 mg (2.66 mmol) of NaI in 30 mL of acetonitrile, a solution of 377 mg (2.66 mmol) of BF₃·Et₂O in 5 mL of acetonitrile was added. After stirring at 25 °C for 12 h the reaction mixture was poured into 100 mL of H₂O and extracted with Et₂O (3 × 25 mL). The organic layer was washed with 10% NaHSO₃ solution (1 × 20 mL), H₂O (1 × 25 mL) and dried over MgSO₄. Evaporation of the solvent at reduced pressure and purification of the residue by flash chromatography (silica gel, hexane) yielded 682 mg (86%) of **1**. ¹H NMR (300 MHz, CDCl₃): δ = 7.51-7.44 (m, 2 H), 7.33-7.25 (m, 2 H), 7.22-7.16 (t, J = 7.4, 2.2 Hz, 1 H), 2.91 (m, 2 H), 2.31-2.20 (m, 2 H), 1.61-1.42 (m, 4 H), 1.21-1.11 (m, 2 H) ppm; ¹³C NMR (CDCl₃, 75 MHz): δ = 146.2, 128.6, 127.2, 126.4, 62.6, 46.9, 32.0, 24.6 ppm; MS (EI, 70 eV) *m/z* (%): 171 (100) [M⁺ - I], 143 (16), 129 (42), 115 (20), 109 (20), 91 (50); UV-Vis (*n*-hexane): λ = 230 (7800), 276 (2300) nm; Elemental analysis (%) calc for C₁₃H₁₅: C 52.37, H 5.07; found: C 52.21, H 5.16.

Compound 2: To a mixture of 8.81 g (20.47 mmol) of PBr₅ and 40 mL of CH₂Cl₂, a solution of 2.57 g (13.65 mmol) of **7** in 10 mL of CH₂Cl₂ was slowly added at 25°C. After 1 h the reaction mixture was washed with H₂O (1 × 30 ml), 10% NaHSO₃ solution (1 × 25 ml) and H₂O (1 ×

30 ml) and was dried over MgSO₄. The solvent was evaporated at reduced pressure and the residue was purified by flash chromatography (silica gel, hexane) to yield 2.81 g (82%) of **2**. ¹H NMR (300 MHz, CDCl₃): δ = 7.51-7.44 (m, 2 H), 7.37-7.18 (m, 3 H), 2.87 (m, 2 H), 2.20-2.40 (m, 2 H), 1.60-1.40 (m, 4 H), 1.40-1.20 (m, 2 H) ppm; ¹³C NMR (CDCl₃, 75 MHz): δ = 143.0, 128.5, 127.5, 126.7, 78.6, 45.2, 30.1, 26.5 ppm; MS (EI, 70 eV) *m/z* (%): 171 (100) [M⁺ - Br], 143 (18), 129 (42), 115 (25), 109 (20), 91 (56), 79 (17), 67 (28); UV-Vis (*n*-hexane): λ = 230 (6200) nm; Elemental analysis (%) calc for C₁₃H₁₅Br: C 62.17, H 6.02; found: C 62.21, H 6.00.

General procedure for the synthesis of chlorides **3 and **5**:** 2.97 ml (41 mmol) of thionyl chloride were slowly added over 13.6 mmol of the corresponding alcohol **7** or **8** at 0°C and the mixture was refluxed for 2 h. The excess of thionyl chloride was distilled at reduced pressure and the residue was purified by flash chromatography (silica gel, pentane) to yield chlorides **3** or **5**.

Compound 3: (98 %); ¹H NMR (300 MHz, CDCl₃): δ = 7.48 (d, 2 H, J = 6.9 Hz), 7.35 (t, 2 H, J = 6.9 Hz), 7.27 (t, 1 H, J = 6.9 Hz), 2.80-2.70 (m, 2 H), 2.35-2.20 (m, 2 H), 1.60-1.40 (m, 4 H), 1.40-1.20 (m, 2 H) ppm; ¹³C NMR (CDCl₃, 75 MHz): δ = 141.7, 128.5, 127.6, 126.9, 82.6, 44.5, 29.1, 27.1 ppm; UV-Vis (*n*-hexane): λ = 219 (8200) nm.

Compound 5: (95 %); ¹H NMR (300 MHz, CDCl₃): δ = 7.45 (td, 1 H, J = 7.8, 1.4 Hz), 7.32-7.24 (m, 1 H), 7.20-7.00 (m, 2 H), 3.08 (q, 1 H, J = 3.9 Hz), 2.82 (t, 1 H, J = 3.7 Hz), 2.35-2.10 (m, 2 H), 1.70-1.20 (m, 6 H) ppm; ¹³C NMR (CDCl₃, 75 MHz): δ = 160.6 (d, J = 248.0 Hz), 129.7 (d, J = 7.9 Hz), 128.9 (d, J = 5.0 Hz), 128.5 (d, J = 13.2 Hz), 124.0 (d, J = 3.1 Hz), 116.6 (d, J = 23.0 Hz), 78.3, 45.1 (d, J = 8.1 Hz), 44.9, 29.1, 28.0, 27.1, 27.0 ppm; MS (EI, 70 eV) *m/z* (%): 226 (3) [M⁺ + 2], 224 (9) [M⁺], 189 (95), 156 (43), 147 (66), 133 (49), 109 (58), 67 (100); Elemental analysis (%) calc for C₁₃H₁₄FCI: C 69.49, H 6.28; found: C 69.38, H 8.73.

General procedure for the synthesis of fluorides **4 and **6**:** A solution of 13.65 mmol of alcohol **7** (or **9**) in 25 mL of CH₂Cl₂ was slowly added at -78°C over 2.20 g (13.65 mmol) of (diethylamino)sulfur trifluoride (DAST) dissolved in 20 mL of CH₂Cl₂. After 1 h at 25 °C the reaction mixture was washed with H₂O (1 × 25 mL) and dried over MgSO₄. Evaporation of the solvent at reduced pressure and purification of the residue by flash chromatography (silica gel, pentane) yielded the corresponding fluoride **4** (or **6**).

Compound 4: (93 %); ¹H NMR (300 MHz, CDCl₃): δ = 7.60-7.52 (m, 2 H), 7.45-7.35 (m, 3 H), 2.60 (m, 2 H), 2.23-2.10 (m, 2 H), 1.55-1.40 (m, 4 H), 1.32-1.21- (m, 2 H); ¹³C NMR (CDCl₃, 75 MHz): δ = 137.3 (d, J = 22.3 Hz), 128.8 (d, J = 3.8 Hz), 128.6 (d, J = 2.8 Hz), 128.0 (d, J = 3.5 Hz), 107.8 (d, J = 188 Hz), 40.7 (d, J = 19 Hz), 28.3 (d, J = 3.1 Hz), 26.5 (d, J = 5.5 Hz); MS (EI, 70 eV) *m/z* (%): 190 (94) [M⁺], 148 (73), 135 (88), 122 (99), 86 (94), 84 (100); UV-Vis (*n*-hexane): λ = 205 (8400) nm; Elemental analysis (%) calc for C₁₃H₁₅F: C 82.07, H 7.95; found: C 82.20, H 7.81.

Compound 6: (95 %); ¹H NMR (300 MHz, CDCl₃): δ = 7.55 (dt, 1 H, J = 7.2, 2.0 Hz), 7.44 (d, 1 H, J = 7.1 Hz), 7.35-7.20 (m, 2 H), 3.00-2.87 (m, 2 H), 2.25-2.10 (m, 2 H), 1.65-1.20 (m, 6 H) ppm; ¹³C NMR (CDCl₃, 75 MHz): δ = 135.0, 134.4 (d, J = 21.7 Hz), 131.5 (d, J = 2.7 Hz), 129.9 (d, J = 3.0 Hz), 129.7 (d, J = 4.5 Hz), 126.3, 107.2 (d, J = 191.2 Hz), 41.0 (d, J = 18.0 Hz), 27.9 (d, J = 3.8 Hz), 26.5, 26.4 (d, J = 5.4 Hz) ppm; MS (EI, 70 eV) *m/z* (%): 226 (4) [M⁺ + 2], 224 (11) [M⁺], 189 (34), 169 (35), 158 (26), 157 (27), 156 (74), 147 (71), 134 (26), 133 (46), 81 (100), 79 (25), 67 (36), 66 (30), 41 (26); Elemental analysis (%) calc for C₁₃H₁₄FCI: C 69.49, H 6.28; found: C 69.56, H 6.15.

Compound 9: (60%); ^1H NMR (300 MHz, CDCl_3): δ = 7.51 (dd, 1 H, J = 8.0, 1.6 Hz), 7.39 (dd, 1 H, J = 7.9, 1.6 Hz), 7.28-7.18 (m, 2 H), 3.05 (br s, 1 H), 2.61 (s, 1 H), 2.50 (br s, 1 H), 2.22-2.10 (m, 2H), 1.80-1.20 (m, 6H) ppm; ^{13}C NMR (CDCl_3 , 75 MHz): δ = 139.1, 133.4, 131.2, 129.4, 128.8, 126.6, 87.6, 42.4, 28.3, 27.5 ppm; MS (EI, 70 eV) m/z (%): 224 (3) [$\text{M}^+ + 2$], 222 (9) [M^+], 187 (21), 167 (20), 154 (15), 139 (100), 77 (30), 55 (50), 41 (20); Elemental analysis (%) calc for $\text{C}_{13}\text{H}_{15}\text{ClO}$: C 70.11, H 6.79; found: C 70.20, H 8.68.

Notes and references

^a Departamento de Química Orgánica, Facultad de Ciencias Químicas. Universidad Complutense de Madrid, Ciudad Universitaria s/n, 28040 Madrid, Spain. E-mail: josio@quim.ucm.es, israel@quim.ucm.es

^b Departamento de Química Física, Facultad de Ciencias Químicas, Universidad Complutense de Madrid, Ciudad Universitaria s/n, 28040 Madrid, Spain.

^c EUIT Forestales, Universidad Politécnica de Madrid, 28040 Madrid, Spain.

^d Laboratorio de difracción de Rayos X, Facultad de Ciencias Químicas, Universidad Complutense de Madrid, Ciudad Universitaria s/n, 28040 Madrid, Spain.

† Electronic Supplementary Information (ESI) available: [Crystallographic data, histograms, UV-Vis spectra, ^1H and ^{13}C spectra and cartesian coordinates and total energies]. See DOI: 10.1039/b000000x/

- 1 a) *Halogen Bonding: Fundamentals and Applications, of Structure and Bonding, Vol. 126* (Eds.: P. Metrangolo and G. Resnati), Springer, Berlin, 2008; b) P. Metrangolo, F. Meyer, T. Pilati, G. Resnati and G. Terraneo, *Angew. Chem. Int. Ed.*, 2008, **47**, 6114; c) P. Metrangolo and G. Resnati, *Cryst. Growth Des.*, 2012, **12**, 5835;
- 2 a) P. Politzer, J. S. Murray and T. Clark, *Phys. Chem. Chem. Phys.*, 2010, **12**, 7748; b) P. Politzer and J. S. Murray *ChemPhysChem*, 2013, **14**, 278.
- 3 A. C. Legon, *Phys. Chem. Chem. Phys.*, 2010, **12**, 7736.
- 4 M. Erdélyi, *Chem. Soc. Rev.*, 2012, **41**, 3547.
- 5 M. Egli and S. Sarkhel, *Acc. Chem. Res.*, 2007, **40**, 197.
- 6 T. J. Mooibroek, P. Gamez and J. Reedijk, *CrystEngComm*, 2008, **10**, 1501.
- 7 J.-J. An, R.-M. Wu, T. Yang, D.-Y. Wu and X. Wang, *Comput. Theor. Chem.*, 2013, **1017**, 144.
- 8 H. Zhuo, Q. Li, W. Li and J. Cheng, *Phys. Chem. Chem. Phys.*, 2014, **16**, 159.
- 9 H. S. El-Sheshtawy, B. S. Bassil, K. I. Assaf, U. Kortz and W. M. Nau, *J. Am. Chem. Soc.*, 2012, **134**, 19935.
- 10 D.-X. Wang, Q.-Y. Zheng, Q.-Q. Wang and M.-X. Wang, *Angew. Chem. Int. Ed.*, 2008, **47**, 7485.
- 11 T. Shirman, T. Arad and M. E. van der Boom, *Angew. Chem. Int. Ed.*, 2010, **49**, 926.
- 12 A. Vargas Jentzsch, D. Emery, J. Mareda, P. Metrangolo, G. Resnati and S. Matile, *Angew. Chem. Int. Ed.*, 2011, **50**, 11675.
- 13 A. Caballero, F. Zapata, N. G. White, P. J. Costa, V. Félix and P. D. Beer, *Angew. Chem. Int. Ed.*, 2012, **51**, 1876.
- 14 H. Y. Gao, X. R. Zhao, H. Wang, X. Pang and W. J. Jin, *Cryst. Growth Des.*, 2012, **12**, 4377.
- 15 B. Ji, W. Wang, D. Deng and Y. Zhang, *Cryst. Growth Des.*, 2011, **11**, 3622.
- 16 H. Y. Gao, Q. J. Shen, X. R. Zhao, X. Q. Yang, X. Pang and W. J. Jin, *J. Mater. Chem.*, 2012, **22**, 5336.
- 17 H. Matter, M. Nazaré, S. Güssregen, D. W. Will, H. Schreuder, A. Bauer, M. Urmann, K. Ritter, M. Wagner and V. Wehner, *Angew. Chem. Int. Ed.*, 2009, **48**, 2911.
- 18 L. A. Hardegger, B. Kuhn, B. Spinnler, L. Anselm, R. Ecabert, M. Stihle, B. Gsell, R. Thoma, J. Díez, J. Benz, J.-M. Plancher, G.

- Hartmann, D. W. Banner, W. Haap and F. Diederich, *Angew. Chem. Int. Ed.*, 2011, **50**, 314.
- 19 A. J. Parker, J. Stewart, K. J. Donald and C. A. Parish, *J. Am. Chem. Soc.*, 2012, **134**, 5165.
- 20 R. Wilcken, X. Liu, M. O. Zimmermann, T. J. Rutherford, A. R. Fersht, A. C. Joerger and F. M. Boeckler, *J. Am. Chem. Soc.*, 2012, **134**, 6810.
- 21 A. Vargas Jentzsch, D. Emery, J. Mareda, S. K. Nayak, P. Metrangolo, G. Resnati, N. Sakai and S. Matile, *Nat. Commun.*, 2012, 3:905 doi: 10.1038/ncomms1902.
- 22 a) Y. Lu, Y. Wang and W. Zhu, *Phys. Chem. Chem. Phys.*, 2010, **12**, 4543; Z. Xu, Z. Yang, Y. Liu, Y. Lu, K. Chen and W. Zhu, *J. Chem. Inf. Model.* 2014, **54**, 69.
- 23 G. J. Bartlett, R. W. Newberry, B. Van Veller, R. T. Raines and D. N. Woolfson, *J. Am. Chem. Soc.*, 2013, **135**, 18682.
- 24 a) L. Brammer, G. Mínguez Espallargas and S. Libri, *CrystEngComm*, 2008, **10**, 1712; b) G. Mínguez Espallargas, F. Zordan, L. A. Marín, H. Adams, K. Shankland, J. van de Streek and L. Brammer, *Chem. Eur. J.*, 2009, **15**, 7554.
- 25 a) T. Clark, M. Hennemann, J. S. Murray and P. Politzer, *J. Mol. Model.*, 2007, **13**, 291; b) P. Politzer, J. S. Murray and M. C. Concha, *J. Mol. Model.*, 2008, **14**, 659; c) J. S. Murray, P. Lane and P. Politzer, *J. Mol. Model.*, 2012, **18**, 541; J. S. Murray, L. Macaveiu, and P. Politzer, *J. Comput. Sci.* 2014, **5**, 590.
- 26 S. V. Rosokha, I. S. Neretin, T. Y. Rosokha, J. Hecht and J. K. Kochi, *Heteroatom Chem.*, 2006, **17**, 449.
- 27 Y.-X. Lu, J.-W. Zou, Y.-H. Wang and Q.-S. Yu, *Int. J. Quantum Chem.*, 2006, **107**, 1479.
- 28 H. G. Wallnoefer, T. Fox, K. R. Liedl and C. S. Tautermann, *Phys. Chem. Chem. Phys.*, 2010, **12**, 14941.
- 29 a) E. Munasamy, R. Sedlak and P. Hobza, *ChemPhysChem*, 2011, **12**, 3253; b) K. E. Riley and P. Hobza, *Phys. Chem. Chem. Phys.*, 2013, **15**, 17742.
- 30 L. P. Wolters and F. M. Bickelhaupt, *ChemistryOpen*, 2012, **1**, 96.
- 31 a) B. Pinter, N. Nagels, W. A. Herrebout and F. De Proft, *Chem. Eur. J.*, 2013, **19**, 519; b) N. Nagels, D. Hauchecorne and W. A. Herrebout, *Molecules* 2013, **18**, 6829.
- 32 J. G. Hill and X. Hu, *Chem. Eur. J.*, 2013, **19**, 3620.
- 33 A. J. Stone, *J. Am. Chem. Soc.*, 2013, **135**, 7005.
- 34 For a recent work on As(lone pair)··· π interactions, see: J. Zukerman-Schpector, A. Otero-de-la-Roza, V. Luaña and E. R. T. Tiekink, *Chem. Commun.*, 2011, **47**, 7608.
- 35 a) Y. Zhang, N. Ma and W. Wang, *Chem. Phys. Lett.*, 2012, **532**, 27. See also: b) C. D. Tatko and M. L. Waters, *Organic Lett.* 2004, **6**, 3969; c) H. Adams, S. L. Cockroft, C. Guardigli, C. A. Hunter, K. R. Lawson, J. Perkins, S. E. Spey, C. J. Urch and R. Ford, *ChemBioChem* 2004, **5**, 657
- 36 For studies on systems with both halogen bonds and lone pair··· π interactions, see: a) Y. Lu, Y. Liu, H. Li, X. Zhu, H. Liu and W. Zhu, *J. Phys. Chem. A*, 2012, **116**, 2591; b) N. Ma, Y. Zhang, B. Ji, A. Tian and W. Wang, *ChemPhysChem*, 2012, **13**, 1411; c) W. Wu, Y. Lu, Y. Liu, H. Li, C. Peng, H. Liu and W. Zhu, *Chem. Phys. Lett.*, 2013, **582**, 49; d) N. Nassirinia, S. Amani, S. J. Teat, O. Roubeau and P. Gomez, *Chem. Commun.*, 2014, **50**, 1003; e) G. Berger, J. Soubhye, A. van der Lee, C. V. Velde, R. Wintjens, P. Dubois, S. Clément and F. Meyer, *ChemPlusChem*, 2014, **79**, 552.
- 37 A. García Martínez, J. Osío Barcina, A. De Fresno Cerezo and R. Gutiérrez Rivas, *J. Am. Chem. Soc.*, 1998, **120**, 673.
- 38 A. García Martínez, J. Osío Barcina and A. de Fresno Cerezo, *Chem. Eur. J.*, 2001, **7**, 1171.
- 39 J. Osío Barcina, I. Fernández and M. R. Colorado Heras, *Eur. J. Org. Chem.*, 2012, 940.
- 40 A. García Martínez, J. Osío Barcina, M. R. Colorado Heras, A. de Fresno Cerezo and M. R. Torres Salvador, *Chem. Eur. J.*, 2003, **9**, 1157.
- 41 A. Rueda-Zubiaurre, N. Herrero-García, M. R. Torres, I. Fernández and J. Osío Barcina, *Chem. Eur. J.*, 2012, **18**, 16884.

- 42 For some examples, see: a) H. Y. Gao, Q. J. Shen, X. R. Zhao, X. Q. Yan, X. Pang and W. J. Jin, *J. Mater. Chem.*, 2012, 5336; b) Q. J. Shen, X. Pang, X. R. Zhao, H. Y. Gao, H.-L. Sun and W. J. Jin, *CrystEngComm*, 2012, 14, 5027; c) H. Matter, M. Nazaré, S. Güssregen, D. W. Will, H. Schreuder, A. Bauer, M. Urmann, K. Ritter, M. Wagner and V. Wehner, *Angew. Chem. Int. Ed.*, 2009, 48, 2911.
- 43 C. J. McAdam, L. R. Hanton, S. C. Moratti and J. Simpson, *Acta Cryst.*, 2009, E65, o1573.
- 44 N. Okamoto, Y. Miwa, H. Minami, K. Takeda and R. Yanada, *J. Org. Chem.*, 2011, 76, 9133.
- 45 M. Zhang, P. Su, X.-G. Meng and X.-M. Xu, *Acta Cryst.*, 2007, E63, o951.
- 46 a) M. Mazik, A. C. Buthe and P. G. Jones, *Tetrahedron*, 2010, 66, 385; b) P. G. Jones, P. Kus and I. Dix, *Z. Naturforsch.*, 2012, 67b, 1273.
- 47 T. J. Mooibroek and P. Gamez, *CrystEngComm*, 2013, 15, 1802. See also reference 6.
- 48 For a review, see: S. V. Rosokha and J. K. Kochi, *X-ray Structures and Electronic Spectra of the π -Halogen Complexes between Halogen Donors and Acceptors with π -Receptors* in Ref. 1, p. 137-160. See also ref. 4.
- 49 a) S. V. Lindeman, J. Hecht and J. K. Kochi, *J. Am. Chem. Soc.*, 2003, 125, 11597; b) S. V. Rosokha, I. S. Neretin, T. Y. Rosokha, J. Hecht and J. K. Kochi, *Heteroatom. Chem.*, 2006, 17, 449; c) Q. J. Shen and W. J. Jin, *Phys. Chem. Chem. Phys.*, 2011, 13, 13721; d) S. V. Rosokha, C. L. Stern and J. T. Ritzert, *Chem. Eur. J.*, 2013, 19, 8774; e) H. Wang, X. R. Zhao and W. J. Jin, *Phys. Chem. Chem. Phys.*, 2013, 15, 4320.
- 50 H.-H. Perkampus, *UV-Vis Atlas of Organic Compounds*, VCH, Weinheim, 1992.
- 51 K. Hirayama, *Handbook of Ultraviolet and Visible Absorption Spectra of Organic Compounds*, Plenum Press, New York, 1967.
- 52 K. Kimura and S. Nagakura, *Spectrochim. Acta*, 1961, 17, 166.
- 53 J. Osío Barcina, N. Herrero-García, F. Cucinotta, L. De Cola, P. Contreras-Carballada, R. M. Williams and A. Guerrero-Martínez, *Chem. Eur. J.*, 2010, 16, 6033.
- 54 N. Herrero-García, I. Fernández and J. Osío Barcina, *Chem. Eur. J.*, 2011, 17, 7327.
- 55 N. Herrero García, M. R. Colorado Heras, M. R. Torres, I. Fernández and J. Osío Barcina, *Eur. J. Org. Chem.*, 2012, 2643.
- 56 D. J. R. Duarte, M. M. de las Vallejos and N. M. Peruchena, *J. Mol. Model.*, 2010, 16, 737.
- 57 See computational Details.
- 58 A referee suggested that the rotation barriers in compounds **5** and **6** may be also affected by H-bonding interactions established between the *ortho* halogen (F or Cl) and the H atom of the tertiary bridgehead carbon of the norbornane moiety (X...H distance around 2 angstroms). This referee suggested to perform some single point calculations using the TS and ground state geometries changing the CH that forms the H bond by a N atom and see if the barrier is affected. In this situation, where the H-bonding interaction is not possible, our calculations reveal that the rotation barriers are not affected significantly (20.3 vs. 19.4 kcal/mol and 11.1 vs. 10.9 kcal/mol, for nitrogen substituted **5** and **6**, respectively) (see Figure S6 in the supplementary information).
- 59 For studies on the relative stability of the conformations of benzylic halides, based on steric repulsions, $\pi \rightarrow \sigma^*$ hyperconjugation (benzylic anomeric effect), $\pi^*-\sigma^*$ interactions and F... π repulsive interactions, see: a) A. Vila, M. García Bugarín and R. A. Mosquera, *J. Phys. Chem. A*, 2011, 115, 13088; b) R. Matsumoto, T. Suzuki and T. Ichimura, *J. Phys. Chem. A*, 2005, 109, 3331; c) K. Utzat, A. A. Restrepo, R. K. Bohn and H. H. Michels, *Int. J. Quantum Chem.*, 2004, 100, 964; d) R. K. Bohn, S. A. Sorenson, N. S. True, T. Brupbacher, M. C. L. Gerry and W. Jäger, *J. Mol. Spectrosc.*, 1997, 184, 167; e) T. Schaefer, R. W. Schurko, R. Sebastian and F. E. Hruska, *Can. J. Chem.*, 1995, 73, 816; f) S. A. Sorenson and N. S. True, *J. Mol. Struct.*, 1991, 263, 21; g) G. Celebre, G. De Luca, M. Longeri and J. W. Emsley, *Molec. Phys.*, 1989, 67, 239; h) G. H. Penner, T. Schaefer, R. Sebastian and S. Wolfe, *Can. J. Chem.*, 1987, 65, 1845; i) W. Adcock and A. N. Abeywickrema, *Aust. J. Chem.*, 1980, 33, 181.
- 60 Gaussian 09, Revision D.01, M. J. Frisch, G. W. Trucks, H. B. Schlegel, G. E. Scuseria, M. A. Robb, J. R. Cheeseman, G. Scalmani, V. Barone, B. Mennucci, G. A. Petersson, H. Nakatsuji, M. Caricato, X. Li, H. P. Hratchian, A. F. Izmaylov, J. Bloino, G. Zheng, J. L. Sonnenberg, M. Hada, M. Ehara, K. Toyota, R. Fukuda, J. Hasegawa, M. Ishida, T. Nakajima, Y. Honda, O. Kitao, H. Nakai, T. Vreven, J. A. Montgomery, Jr., J. E. Peralta, F. Ogliaro, M. Bearpark, J. J. Heyd, E. Brothers, K. N. Kudin, V. N. Staroverov, R. Kobayashi, J. Normand, K. Raghavachari, A. Rendell, J. C. Burant, S. S. Iyengar, J. Tomasi, M. Cossi, N. Rega, J. M. Millam, M. Klene, J. E. Knox, J. B. Cross, V. Bakken, C. Adamo, J. Jaramillo, R. Gomperts, R. E. Stratmann, O. Yazyev, A. J. Austin, R. Cammi, C. Pomelli, J. W. Ochterski, R. L. Martin, K. Morokuma, V. G. Zakrzewski, G. A. Voth, P. Salvador, J. J. Dannenberg, S. Dapprich, A. D. Daniels, Ö. Farkas, J. B. Foresman, J. V. Ortiz, J. Cioslowski, and D. J. Fox, Gaussian, Inc., Wallingford CT, 2009.
- 61 Y. Zhao and D. G. Truhlar, *Acc. Chem. Res.*, 2008, 41, 157.
- 62 F. Weigend and R. Alhrichs, *Phys. Chem. Chem. Phys.*, 2005, 7, 3297.
- 63 a) M. E. Casida, *Recent Developments and Applications of Modern Density Functional Theory*, Vol. 4, Elsevier, Amsterdam, 1996; b) M. E. Casida and D. P. Chong, *Recent Advances in Density Functional Methods*, Vol. 1, World Scientific, Singapore, 1995, p. 155.
- 64 a) A. D. Becke, *J. Chem. Phys.*, 1993, 98, 5648; b) C. Lee, W. Yang and R. G. Parr, *Phys. Rev. B*, 1988, 37, 785.
- 65 a) S. Miertuš, E. Scrocco and J. Tomasi, *Chem. Phys.*, 1981, 55, 117; b) J. L. Pascual-Ahuir, E. Silla and I. Tuñón, *J. Comp. Chem.*, 1994, 15, 1127; c) V. Barone and M. Cossi, *J. Phys. Chem. A*, 1998, 102, 1995.
- 66 For a review, see: a) A. Dreuw and M. Head-Gordon, *Chem. Rev.*, 2005, 105, 4009.
- 67 a) J. P. Foster and F. Weinhold, *J. Am. Chem. Soc.*, 1980, 102, 7211. b) A. E. Reed and F. J. Weinhold, *J. Chem. Phys.*, 1985, 83, 1736. c) A. E. Reed, R. B. Weinstock and F. Weinhold, *J. Chem. Phys.*, 1985, 83, 735. d) A. E. Reed, L. A. Curtiss and F. Weinhold, *Chem. Rev.*, 1988, 88, 899.